

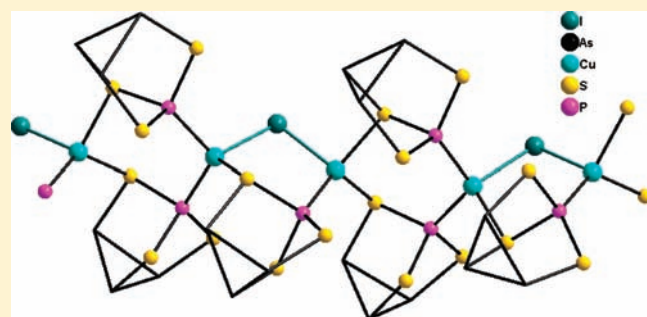
PA₃S₃ Cage as a New Building Block in Copper Halide Coordination Polymers

Patrick Schwarz, Joachim Wachter,* and Manfred Zabel

Institut für Anorganische Chemie, Universität Regensburg, D-93040 Regensburg, Germany

Supporting Information

ABSTRACT: First examples of the coordination chemistry of the PA₃S₃ cage were obtained from solutions of PA₃S₃·W(CO)₅ (**1**) in CH₂Cl₂ or CH₂Cl₂/toluene and CuX (X = Cl, Br, I) in MeCN through interdiffusion techniques. Crystals of [Cu(PA₃S₃)₄]X (**2**, X = Cl; **3**, X = Br) and [(Cu₂I)(PA₃S₃)₃]I (**4**) were obtained and characterized by Raman spectroscopy (**2**) and single-crystal X-ray crystallography. The solid-state structures reveal an unexpected coordination versatility of the PA₃S₃ ligand: apical phosphorus and bridging sulfur atoms interact with copper, while As···X interactions determine the dimensionality of the frameworks. The structures of **2** and **3** contain tetrahedral [(PA₃S₃)₄Cu]⁺ cations as secondary building units (SBUs), which are arranged by interactions with Cl[−] or Br[−] anions into two- and three-dimensional substructures. These interpenetrate into a (2D + 3D) polycatenane. Compound **4** is built up by a one-dimensional [(Cu₂I)(PA₃S₃)₃]ⁿ⁺ ribbon with PA₃S₃ cages as P,S-linkers. The As atoms of the exo PA₃S₃ linkers interact with iodide counterions (3.35 < d(As–I) < 3.59 Å). The resulting two-dimensional layer is organized by weak As···I interactions (d(As–I) = 3.87 Å) into a 3D network.



INTRODUCTION

As₄S₃ as well as P₄S₃ are cage molecules of the nortricyclane type.¹ The coordination behavior of P₄S₃ toward Lewis-acid compounds is already well established because of its better solubility in organic solvents.² Recently, we have shown that both compounds form structurally very different coordination polymers with copper halides.³ Whereas P₄S₃ coordinates exclusively through its P atoms,⁴ As₄S₃ interacts with copper through sulfur.⁵ In the latter case formation of three-dimensional networks seems to be additionally supported by weak but significant As–X (X = Cl, Br, I) interactions. These differences cannot be explained by theoretical studies. Density functional theory calculations on P₄S₃⁶ and As₄S₃ do not show significant differences in the energy and shape of HOMOs and LUMOs.⁷

A chemical approach for solution of this problem could be the investigation of the yet unknown coordination behavior⁸ of mixed cages P_nAs_{4–n}S₃ (n = 1–3).⁹ Of particular interest may be the PA₃S₃ cage, because it combines the PS₃ building block of P₄S₃ and the As₃ basis of As₄S₃.¹⁰ This similarity makes it an interesting ligand for the formation of coordination polymers with copper(I) halides. In this work we report on the formation of novel coordination polymers of PA₃S₃ via participation of P and S coordination sites, while the As sites are blocked by intermolecular interactions with halide ions.

RESULTS AND DISCUSSION

1. Synthesis and Characterization of PA₃S₃·W(CO)₅ (**1**).

The high-temperature synthesis from the elements was reported to give PA₃S₃ along with phosphorus-rich P_nAs_{4–n}S₃ (n = 2–4) compounds.^{9a} We found that fusing together stoichiometric amounts of P, As, and S at 600 °C for 7 days followed by extremely slow cooling (1 °C/min) to room temperature gave yellow-orange PA₃S₃ of spectroscopic purity. The ³¹P NMR spectrum in CS₂ (δ = 104 ppm) is in agreement with formation of P_{apical}As₃S₃.¹¹ However, the ³¹P MAS NMR spectrum reveals two singlets of equal intensity at δ = 106 and 113 ppm. The existence of two phosphorus resonances may be explained by a different orientation of the cage molecules in the crystal. This phenomenon was first described for β-P₄S₃¹² and was also found for P₄Se₃.¹³ Because of the extremely low solubility of PA₃S₃ in, e.g., toluene, CH₂Cl₂, and THF we investigated formation of an adduct with W(CO)₅. In analogy to the chemistry of As₄S₃, such an adduct should be much more soluble.⁵

Reaction of PA₃S₃ with W(CO)₅·THF in THF gave after filtration over SiO₂ PA₃S₃·W(CO)₅ (**1**) as a yellow-orange powder in 52% yield. The IR spectrum reveals absorptions at 1935 and 2080 cm^{−1} which are characteristic of ν(CO) stretch

Received: May 19, 2011

Published: July 28, 2011

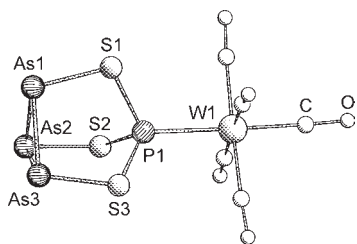
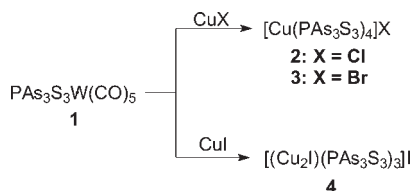


Figure 1. Molecular structure of $\text{PAs}_3\text{S}_3 \cdot \text{W}(\text{CO})_5$ (**1**). Selected distances (Å): P1–S1 2.095(1), P1–S2 2.097(1), P1–S3 2.091(1), As1–S1 2.190(1), As2–S2 2.203(1), As3–S3 2.181(1), As1–As2 2.438(1), As1–As3 2.417(1), As2–As3 2.429(1), P1–W1 2.460(1).

Scheme 1. Diffusion Reactions of 1 (in toluene or/and CH_2Cl_2) with CuX ($\text{X} = \text{Cl}, \text{Br}, \text{I}$) (in MeCN)



vibrations typical of a $\text{W}(\text{CO})_5$ fragment. The field desorption mass spectrum exhibits the parent ion at $m/z = 675.6$. The ^{31}P NMR spectrum in C_6D_6 shows a singlet at $\delta = 115.9$ ppm. The observed $^1\text{J}_{\text{P,W}}$ coupling of 300 Hz is stronger than that in $\text{P}_4\text{S}_3 \cdot \text{W}(\text{CO})_5$ (126 Hz).¹⁴ The ^{31}P MAS NMR spectrum contains one signal at $\delta = 113.0$ ppm and weak resonances at $\delta = 109$ and -64.3 ppm indicating impurities of still unknown nature. The structure of **1** is composed of a PAs_3S_3 cage bearing a $\text{W}(\text{CO})_5$ fragment at the apical P atom (Figure 1). There are no significant distortions within the cage compared to the free molecule.^{10a} Only the As–S bonds are slightly lengthened by 0.02–0.04 Å. The packing in the crystal structure may be described by layers parallel to the ab plane but with an inverse orientation of the $\text{W}(\text{CO})_5$ groups in neighbored layers (Figure S1, Supporting Information).

2. Synthesis and Characterization of Coordination Polymers. **2.1. Syntheses and Spectroscopic Data.** Layering of solutions of **1** in the respective solvent with solutions of copper(I) halides gave after complete interdiffusion yellow crystals (ca. 1% yield) of $[\text{Cu}(\text{PAs}_3\text{S}_3)_4]\text{Cl}$ (**2**), $[\text{Cu}(\text{PAs}_3\text{S}_3)_4]\text{Br}$ (**3**), and $[(\text{Cu}_2\text{I})(\text{PAs}_3\text{S}_3)_3]\text{I}$ (**4**) (Scheme 1). The low yields may be explained by competitive formation of yellow, orange, or brown powders during the diffusion process. Formation of crystals is solvent dependent. Thus, **2** crystallizes from solutions of **1** in toluene, crystallization of **3** occurs when using a mixture of **1**, toluene, and CH_2Cl_2 , and **4** requires dissolution of **1** in CH_2Cl_2 . Variation of the stoichiometry and concentration did not affect the crystallization processes. Layering of saturated solutions of PAs_3S_3 in toluene, CH_2Cl_2 , or CS_2 with CuX solutions gave in all cases immediate precipitation of powders at the phase border.

For the purpose of comparison, reaction of a hot saturated solution of PAs_3S_3 in toluene with CuCl in CH_3CN was studied. An orange microcrystalline material precipitated in nearly quantitative yield. The Raman spectrum of this material agrees fairly well with the spectrum of pure **2** (Figure S2, Supporting

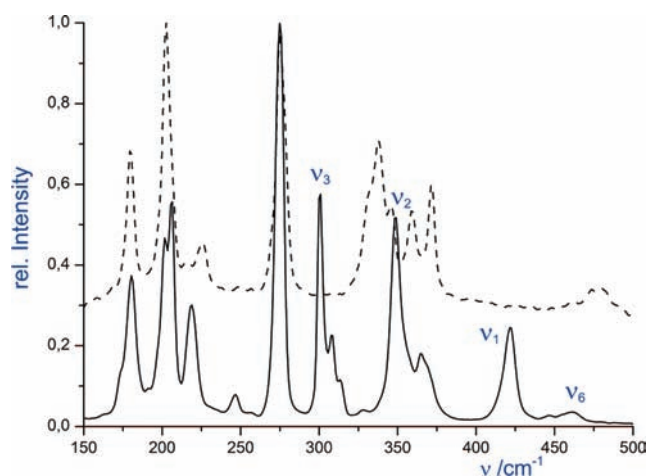


Figure 2. Raman spectra of PAs_3S_3 (—) and $[\text{Cu}(\text{PAs}_3\text{S}_3)_4]\text{Cl}$ (**2**) (---).

Table 1. Raman Frequencies [cm^{-1}] of PAs_3S_3 and $[\text{Cu}(\text{PAs}_3\text{S}_3)_4]\text{Cl}$ (2**)**

PAs_3S_3 ¹⁵	assignment ¹⁵	PAs_3S_3 ^a	2
183m	ν_{10} (E)	180m	179m
206s	ν_8 (E)	206s	202vs
223m	ν_9 (E)	218m	225w
243w		246w	247vw
277s	ν_4 (A_1)	274vs	274vs
312m	ν_3 (A_1)	307s	
354vs	ν_2 (A_1)	349s	337s, 346sh
		364sh	358w, 371 m
424mw	ν_1 (A_1)	421m	
464w	ν_6 (E)	461w,br	479w,br

^aThis work.

Information). Therefore, similar composition and structures for both products are very likely.

Raman spectra of PAs_3S_3 and **2** were measured (Figure 2). The comparison of both spectra shows that the frequencies ν_1 , ν_3 , and ν_6 of the free cage, which are assigned to vibrations of the apical PS_3 moiety,¹⁵ are significantly affected, very likely by coordination to copper (Table 1). The mode ν_2 (symmetric As–S stretching) of the free cage is split into vibrations at 337, 346, 358, and 371 cm^{-1} . The interaction of the As_3 basis with the Cl^- anion is held responsible for this splitting (see below), although it is difficult to assign the vibrations. A similar influence of copper coordination on P_4S_3 Raman frequencies has been studied recently.¹⁴

2.2. Structures of $[\text{Cu}(\text{PAs}_3\text{S}_3)_4]\text{X}$ ($\text{X} = \text{Cl}, \text{Br}$). The structures of **2** and **3** are composed of pairs of $[(\text{PAs}_3\text{S}_3)_4\text{Cu}]^+$ cations and Cl^- or Br^- anions. The cations are built up of a central copper atom, which is tetrahedrally surrounded by four apical P atoms of PAs_3S_3 molecules (Figure 3). The Cu–P distances (2.23–2.27 Å) are in the same range as those observed for copper phosphides.¹⁶

The crystal structures of **2** (and isostructural **3**) were determined by interactions between As_3 basis atoms and Cl^- (Br^-) anions, Table 2. In the structure of **2** there are two different types A and B of $[(\text{PAs}_3\text{S}_3)_4\text{Cu}]^+$ cations, which are defined by the number of Cl^- anions interacting with PAs_3S_3 cages. In type A

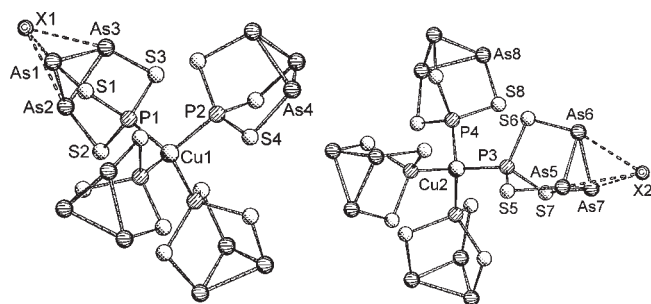


Figure 3. Structure of $[\text{Cu}(\text{PAs}_3\text{S}_3)_4]\text{X}$ ($\text{X} = \text{Cl}, 2, \text{Br}, 3$). The two different cations with the corresponding anions are shown.

Table 2. Selected Distances (Å) of $[\text{Cu}(\text{PAs}_3\text{S}_3)_4]\text{X}$ ($\text{X} = \text{Cl}, 2, \text{Br}, 3$)

	2	3
Cu1–P1	2.229(4)	2.225(3)
Cu1–P2	2.235(7)	2.240(5)
Cu2–P3	2.271(4)	2.291(2)
Cu2–P4	2.229(11)	2.237(7)
P1–S1	2.069(6)	2.072(4)
P1–S2	2.076(6)	2.066(4)
P1–S3	2.086(7)	2.068(5)
P2–S4	2.078(4)	2.074(3)
P3–S5	2.082(7)	2.061(5)
P3–S6	2.078(7)	2.065(5)
P3–S7	2.077(6)	2.067(4)
P4–S8	2.097(10)	2.075(8)
As1–S1	2.243(3)	2.233(6)
As2–S2	2.233(6)	2.220(5)
As3–S3	2.242(6)	2.232(5)
As4–S4	2.236(4)	2.230(3)
As5–S5	2.245(5)	2.256(4)
As6–S6	2.235(6)	2.239(4)
As7–S7	2.243(5)	2.256(4)
As8–S8	2.201(8)	2.210(6)
As1–As2	2.473(3)	2.474(2)
As1–As3	2.483(3)	2.482(2)
As2–As3	2.473(3)	2.466(2)
As4–As4a	2.496(3)	2.481(2)
As5–As6	2.471(4)	2.461(3)
As5–As7	2.476(3)	2.464(2)
As6–As7	2.464(3)	2.448(3)
As8–As8a	2.472(15)	2.457(10)

cations four PAs_3S_3 molecules are arranged around one Cl^- anion with $\text{As}\cdots\text{Cl}$ distances between 3.14 and 3.18 Å (Figure 4), whereas in type B cations there are only three PAs_3S_3 molecules with $\text{As}\cdots\text{Cl}$ distances between 3.13 and 3.20 Å (Figure 5). The observed $\text{As}\cdots\text{Cl}$ distances are significantly shorter than the sum of the van der Waals radii of As and Cl. The corresponding $\text{As}\cdots\text{Br}$ distances in 3 range from 3.24 to 3.37 Å in both types of cations.

Two different substructures of different dimensionality follow from the different coordination pattern of Cl^- anions: Cation A interacts with four Cl^- anions of coordination number 12,

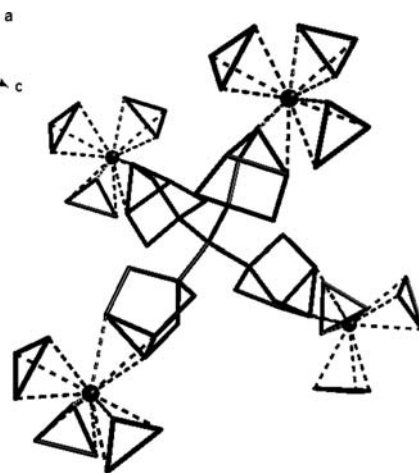


Figure 4. Section of the 3D network of 2 represented by cation 2A and corresponding $\text{As}\cdots\text{Cl}$ interactions (---). Each Cl^- anion is surrounded by four PAs_3S_3 molecules, but only one of them is shown completely for the sake of clarity.

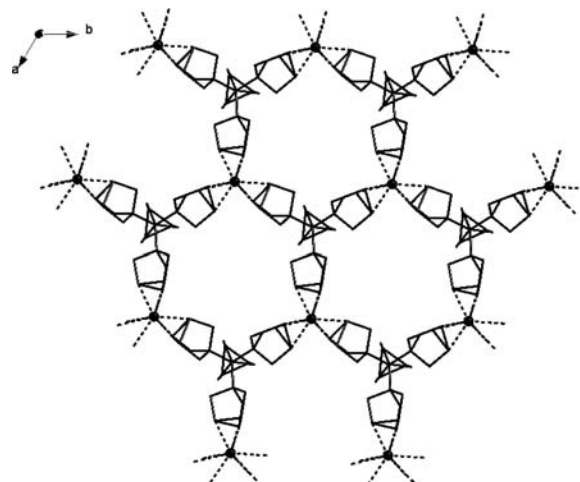


Figure 5. Section of the 2D network of 2 represented by cation B and corresponding $\text{As}\cdots\text{Cl}$ interactions (---).

leading to formation of a 3D network (Figure 4). In the second substructure cation B interacts with three Cl^- anions of coordination number 9, giving rise to a 2D network parallel to ab . The cage without interaction with Cl^- is oriented along c . A further characteristic of this cage is large thermal ellipsoids, which is in agreement with a possible motion in the crystal lattice (Figure 5). The two-dimensional layer possesses voids with an average diameter of ca. 10.7 Å. These voids are penetrated by the three-dimensional network, giving a polycatenated structure (Figure 6). Only a few examples of (2D + 3D) polycatenation of substructures of different dimensionality have been described in the literature.¹⁷

2.3. Structure of $[(\text{Cu}_2\text{I})(\text{PAs}_3\text{S}_3)_3]$. Compound 4 is a coordination polymer, which is composed of cationic $[(\text{Cu}_2\text{I})(\text{PAs}_3\text{S}_3)_3]^+$ and anionic (I^-) building blocks (Figure 7). Cationic $[\text{Cu}_2\text{I}(\mu\text{-PAs}_3\text{S}_3)]^+$, which contains a rare example of a cationic copper halide building block,¹⁸ functions as a secondary building unit (SBU). The resulting SBUs are P,S-linked by two cage molecules, giving rise to formation of a one-dimensional

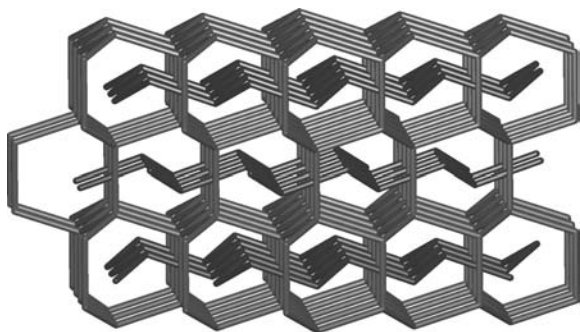


Figure 6. Schematic representation of the (2D + 3D) polycatenation of 2 (and 3).

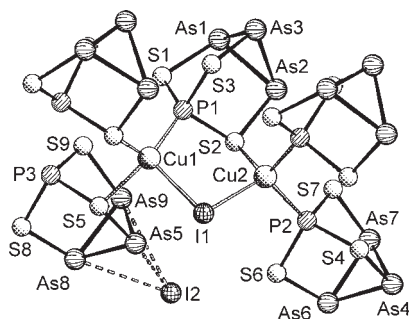


Figure 7. Section of the structure of $[(\text{Cu}_2\text{I})(\text{PAS}_3\text{S}_3)_3]\text{I}$ (4).

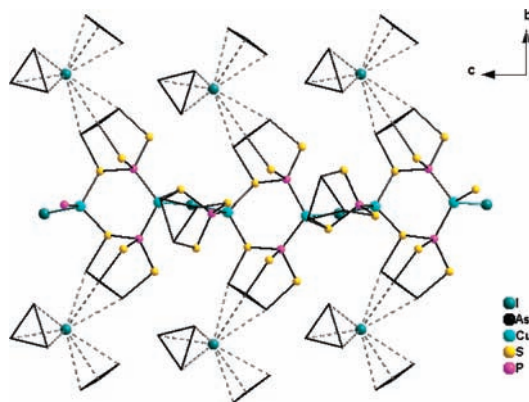


Figure 8. Section of the 1D- $(\text{Cu}_2\text{I})(\text{PAS}_3\text{S}_3)_3$ ribbons with adjacent iodide counterions in 4 and $\text{As}\cdots\text{I}$ interactions $< 3.6 \text{ \AA}$ (---). For the sake of clarity, the exo PAS_3S_3 cages are represented by triangles for the As_3 basis atoms.

$[(\text{Cu}_2\text{I})(\text{PAS}_3\text{S}_3)_3]^{n+}$ ribbon (Figure 8). It is noteworthy that a P,S-coordination behavior of a P_4S_3 -derived cage has been reported thus far only for Ag^+ compounds.^{2g,12}

Coordination of Cu1 is achieved by two S atoms, one P atom, and one iodide ligand, while Cu2 bears iodide, one S atom, and two P atoms. The Cu–S and Cu–I distances are in the range typical of other P_4Q_3 ($\text{Q} = \text{S}, \text{Se}$) coordination polymers with copper(I) iodide,^{4a} just as the Cu–P distances.^{4,16} The distances P1–S2, P2–S4, and P3–S5 are slightly longer than the other P–S distances because of the bridging character of these atoms (Table 3). The As–S and As–As bonds are longer by

Table 3. Selected Distances (\AA) of $[(\text{Cu}_2\text{I})(\text{PAS}_3\text{S}_3)_3]\text{I}$ (4)

Cu1–I1	2.628(3)
Cu2–I1	2.577(3)
Cu1–P1	2.236(5)
Cu2–P2	2.266(4)
Cu2–P3	2.243(4)
Cu1–S4	2.329(4)
Cu1–S5	2.317(4)
Cu2–S2	2.351(4)
P1–S1	2.098(6)
P1–S2	2.112(5)
P1–S3	2.087(6)
P2–S4	2.104(5)
P2–S6	2.084(6)
P2–S7	2.090(5)
P3–S5	2.120(5)
P3–S8	2.086(6)
P3–S9	2.069(6)
As1–S1	2.257(4)
As2–S2	2.278(4)
As3–S3	2.250(5)
As4–S4	2.273(4)
As5–S5	2.278(4)
As6–S6	2.264(4)
As7–S7	2.246(4)
As8–S8	2.258(4)
As9–S9	2.255(4)
As1–As2	2.482(3)
As1–As3	2.465(3)
As2–As3	2.481(3)
As4–As6	2.480(2)
As4–As7	2.478(3)
As6–As7	2.476(3)
As5–As8	2.480(2)
As5–As9	2.477(3)
As8–As9	2.483(3)

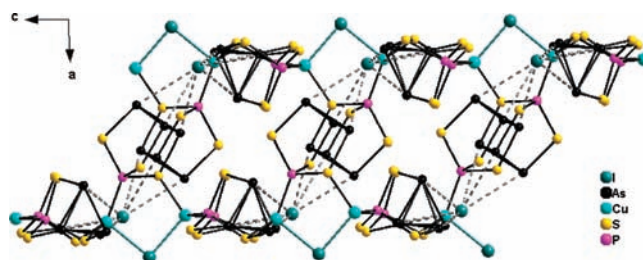


Figure 9. Two-dimensional arrangement of two planar substructures of 4. $\text{As}\cdots\text{I}$ interactions ($3.35 < d < 3.59 \text{ \AA}$) are represented by dashed lines.

$0.03\text{--}0.06 \text{ \AA}$ than those in free PAS_3S_3 ,^{9a} probably as a consequence of weak interactions with the counterions (see below).

The exo As atoms As4–As9 of the 1D- $[(\text{Cu}_2\text{I})(\text{PAS}_3\text{S}_3)_3]^{n+}$ ribbons interact with adjacent iodide counterions to form a layer within the bc plane (Figure 8). The corresponding As–I distances are between 3.35 and 3.59 \AA . This is longer than

covalent As–I bonds, e.g., 2.51 Å in AsI_3 ¹⁹ or 3.05 Å in $\text{As}_6\text{I}_8^{2-}$ ²⁰ but in the same range as weak interlayer As···I interactions in AsI_3 ($d(\text{As}–\text{I}) = 3.5$ Å).¹⁹ Such weak interactions may be forced by electrostatic attractions as observed in $[\text{Cp}^*\text{Fe}_2\text{As}_2\text{Se}_2]\text{I}$ ($d(\text{As}–\text{I}) = 3.24$ Å).²¹

The atoms As1, As2, and As3 of the bridging SBUs coordinate to I2 in the same range, which gives pairs of mutually arranged layers of about 13 Å diameter (Figure 9). Slightly weaker As···I interactions ($d = 3.87$ Å) exist between I1 of each of the $[\text{Cu}_2\text{I}]^+$ units and two As atoms (As6, As8) of PAS_3S_3 molecules

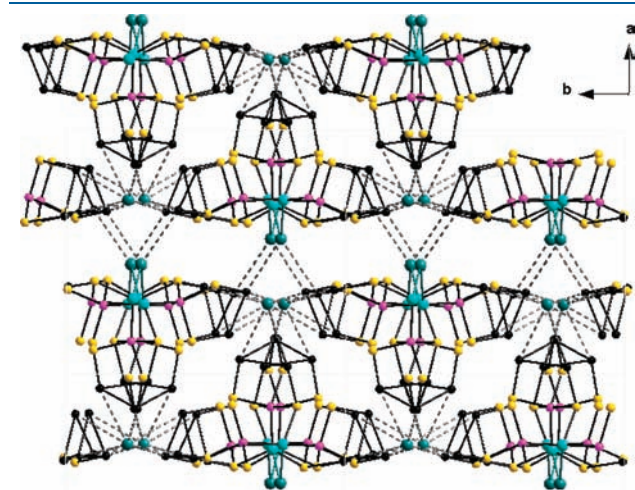


Figure 10. Stacks of planar substructures of **4**, organized by weak As···I interactions ($d = 3.87$ Å).

belonging to the next layer. These distances are still shorter than the sum of the van der Waals radii of As and I (4.15 Å). Finally, a 3D network is built up consisting of stacks of planar substructures parallel to the *bc* plane (Figure 10).

CONCLUSIONS

The first examples of coordination polymers from PAS_3S_3 or its metal carbonyl derivative $\text{PAS}_3\text{S}_3 \cdot \text{W}(\text{CO})_5$ (**1**) and copper halides were obtained by interdiffusion techniques between solvents of different polarity. The solid-state structures demonstrate an unexpected coordination behavior of the PAS_3S_3 building block exhibiting properties in between P_4S_3 and As_4S_3 . Thus, coordination of apical phosphorus is reminiscent of that of P_4S_3 , and weak but significant As···X interactions resemble those of As_4S_3 . However, the role of sulfur, which serves for the first time as a coordination site toward copper, is unprecedented in the series of P_4Q_3 (Q = S, Se) cage molecules.

EXPERIMENTAL SECTION

General Methods. All manipulations were carried out under nitrogen using glovebox or Schlenk techniques. The Raman spectra were recorded on a Varian FTS 7000e spectrometer containing a FT Raman unit. Excitation of the microcrystalline samples was carried out with a Nd:YAG laser ($\lambda = 1064$ nm), and detection was performed with a liquid N_2 -cooled Ge detector. ³¹P MAS NMR spectra were recorded with a Bruker Avance 300 spectrometer using a double-resonance 2.5 mm MAS probe. The ³¹P resonance was 121.495 MHz. All spectra were acquired at a MAS rotation frequency of 30 kHz, a 90° pulse length of 2.3 μs, and a relaxation delay of 450 s.

Table 4. Crystallographic Data of Compounds **1–4**

	1	2	3	4
formula	$\text{C}_2\text{As}_3\text{O}_3\text{PS}_3\text{W}$	$\text{As}_{12}\text{ClCuP}_4\text{S}_{12}$	$\text{As}_{12}\text{BrCuP}_4\text{S}_{12}$	$\text{As}_9\text{Cu}_2\text{I}_2\text{P}_3\text{S}_9$
M_w	675.83	1506.76	1551.21	1436.72
crystal size [mm]	$0.070 \times 0.051 \times 0.042$	$0.13 \times 0.12 \times 0.05$	$0.11 \times 0.044 \times 0.03$	$0.07 \times 0.05 \times 0.01$
crystal system	orthorhombic	trigonal	trigonal	monoclinic
space group	<i>Pbcn</i>	<i>P31c</i>	<i>P31c</i>	<i>P2_1/c</i>
<i>a</i> [Å]	10.594(1)	13.314(1)	13.414(1)	12.020(1)
<i>b</i> [Å]	22.909(1)	13.314(1)	13.414(1)	13.774(1)
<i>c</i> [Å]	12.036(1)	21.172(1)	21.482(1)	15.895(1)
β [deg]				91.7(1)
γ [deg]		120.0	120.0	
<i>V</i> [Å ³]	2921.1(3)	3250.2(2)	3347.7(1)	2630.4(2)
<i>Z</i>	8	4	4	4
σ_{calcd} [g cm ⁻³]	3.073	3.079	3.078	3.628
μ [Cu K α , mm ⁻¹]	27.368	24.411	24.364	41.411
instrument	Oxf. Diff. Gemini Ultra	Oxf. Diff. Gemini Ultra	Oxf. Diff. SuperNova	Oxf. Diff. Gemini Ultra
<i>T</i> [K]	123	123	295	123
scan range	$4.60 < \Theta < 66.49$	$3.83 < \Theta < 66.47$	$3.80 < \Theta < 71.35$	$3.68 < \Theta < 56.23$
reflns collected	9111	8478	16 127	6840
unique obd [$I > 2\sigma(I)$]	2106	2739	4029	2579
params refined	163	182	182	226
abs corr	analytical	analytical	analytical	semiempirical
transmission	0.474/0.274	0.328/0.051	0.412/0.153	1.0000/0.2858
max/min residual density [e/Å ⁻³]	2.424/−2.224	1.518/−0.920	0.586/−0.603	2.581/−2.195
R_1, wR_2 ($I > 2\sigma$)	0.043, 0.136	0.046, 0.116	0.034, 0.095	0.057, 0.154
R_1, wR_2 (all data)	0.051, 0.142	0.047, 0.117	0.035, 0.096	0.073, 0.162

Synthesis of PAs_3S_3 ^{9a}. A 0.4 g (0.013 mmol) amount of red phosphorus, 2.9 g (0.039 mmol) of arsenic, and 1.2 g (0.039 mmol) of sulfur were heated in evacuated vials at 600 °C for 7 days. After very slow cooling (1 °C/min) to room temperature orange PAs_3S_3 is obtained quantitatively. ³¹P MAS NMR (121 MHz): $\delta = 106$ (s), 113 ppm (s).

$\text{PAs}_3\text{S}_3 \cdot \text{W}(\text{CO})_5$. A 50 mL amount of a $\text{W}(\text{CO})_5$ THF solution ($c = 0.028 \text{ mol} \cdot \text{L}^{-1}$) was added to 350 mg (0.99 mmol) of PAs_3S_3 . The resulting suspension was stirred for 18 h at room temperature. After evaporation of the solvent, the residue was dissolved in 25 mL of toluene and filtered over SiO_2 (column 15 × 3 cm). **1** was isolated as a yellow solid, which after washing with pentane was employed for the reactions. Recrystallization from 10 mL of toluene/pentane 2:1 at -24 °C gave material suitable for X-ray diffraction analysis. [$\text{PAs}_3\text{S}_3 \cdot \text{W}(\text{CO})_5$] (**1**): Yield, 348 mg (52%); ³¹P NMR (121 MHz, C_6D_6) $\delta = 115.9$ ppm (s) ($J_{\text{P,W}} = 300$ Hz); ³¹P MAS NMR (121 MHz) $\delta = 113$ ppm; FD MS (toluene) $m/z = 675.6$ (M^+); IR (KBr, cm^{-1}) 1935vs, 2080s [$\nu(\text{CO})$].

Syntheses of $[\text{Cu}(\text{PAs}_3\text{S}_3)_4]\text{Cl}$. *Method A.* A yellow solution of 40 mg (0.059 mmol) of **1** in 20 mL of toluene was layered with a solution of 15 mg (0.15 mmol) of CuCl in 15 mL of acetonitrile. A brown precipitate formed after 2 days; crystallization of yellow prisms started after 4 days. After decantation of the solvent the crystals were washed with toluene and pentane. The composition of the prisms was determined by X-ray diffraction analysis as $[\text{Cu}(\text{PAs}_3\text{S}_3)_4]\text{Cl}$ (**2**).

Method B. A 50 mg (0.14 mmol) amount of PAs_3S_3 was stirred for 1 h at 110 °C in 100 mL of toluene and then filtered. The hot filtrate was combined with a solution of 10 mg (0.1 mmol) of CuCl in 10 mL of acetonitrile. Immediately, a yellow-orange precipitate formed. Crystallization was completed after keeping the solution for 1 day at room temperature to give 45 mg of a microcrystalline powder, which was isolated by decantation of the solvent and washing with pentane. The product was examined Raman spectroscopically. $[\text{Cu}(\text{PAs}_3\text{S}_3)_4]\text{Cl}$ (**2**): Raman (cm^{-1}) 179m, 203s, 224w, 249vw, 278vs, 298vw, 337m, 347w, 357vw, 371 m, 480w,br. Anal. Calcd: S, 25.54. Found: S, 23.51.

$[\text{Cu}(\text{PAs}_3\text{S}_3)_4]\text{Br}$ (3**).** The solution of 25 mg (0.037 mmol) of **1** in a mixture of 30 mL of toluene/ CH_2Cl_2 (v/v 2:1) was layered with a solution of 15 mg (0.1 mmol) of CuBr in 15 mL of acetonitrile. A yellow precipitate formed immediately at the phase border; yellow intergrown crystals formed after 3 days of diffusion. These were separated from yellow powder by decantation and washing with pentane. X-ray diffraction analysis showed them to have composition $[\text{Cu}(\text{PAs}_3\text{S}_3)_4]\text{Br}$ (**3**).

$[(\text{Cu}_2\text{I})(\text{PAs}_3\text{S}_3)_3]\text{I}$ (4**).** A solution of 37 mg (0.055 mmol) of **1** in 25 mL of CH_2Cl_2 was layered with 36 mg (0.19 mmol) of CuI in 20 mL of acetonitrile. A yellow to orange precipitate formed immediately, and then very slowly intergrown yellow platelets crystallized. The reaction was finished after the initially yellow solution of **1** decolorized. After isolation and washing with pentane the crystals were determined to have composition $[(\text{Cu}_2\text{I})(\text{PAs}_3\text{S}_3)_3]\text{I}$ (**4**).

X-ray Structure Determination of Compounds 1–4. Crystallographic data of the crystal structure determinations for **1–4** are given in Table 4. The structures were solved by direct methods (SIR-97 program)²² and refined by full-matrix anisotropic least-squares (SHELXL97 program)²³ with all reflections. The examined crystal of compound **3** was a merohedral twin, the twin law was (-1 0 0, 0 -1 0, 0 0 1), and the ratio of the twin components was refined to 0.616(0.002) to 0.384.

ASSOCIATED CONTENT

Supporting Information. X-ray crystallographic data in CIF format, packing diagram of **1**, and Raman spectrum of microcrystalline **2**. This material is available free of charge via the Internet at <http://pubs.acs.org>.

AUTHOR INFORMATION

Corresponding Author

*Fax: +49-941/943-4439. E-mail: Joachim.Wachter@chemie.uni-regensburg.de.

ACKNOWLEDGMENT

This work was supported by the Deutsche Forschungsgemeinschaft (Wa 486/11-1). We gratefully acknowledge continuous support by Prof. Dr. M. Scheer. We also thank Dr. M. Schlosser for recording the Raman spectra and Dr. C. Gröger for recording the ³¹P MAS NMR spectra.

REFERENCES

- (1) (a) Whitfield, H. J. *J. Chem. Soc. A* **1970**, 1800. (b) Whitfield, H. J. *J. Chem. Soc., Dalton Trans.* **1973**, 1737. (c) Chattopadhyay, T. K.; May, W.; von Schnering, H. G.; Pawley, G. S. *Z. Kristallogr.* **1983**, *165*, 47.
- (2) (a) Cordes, A. W.; Joyner, R. D.; Shores, R. D.; Dill, E. D. *Inorg. Chem.* **1974**, *13*, 132. (b) Jefferson, R.; Klein, H. F.; Nixon, J. F. *J. Chem. Soc., Chem. Commun.* **1969**, 536. (c) Di Vaira, M.; Peruzzini, M.; Stoppioni, P. *J. Organomet. Chem.* **1983**, *258*, 373. (d) Di Vaira, M.; Peruzzini, M.; Stoppioni, P. *Inorg. Chem.* **1983**, *258*, 373. (e) Aubauer, C.; Irran, E.; Klapötke, T. M.; Schnick, W.; Schulz, A.; Senker, J. *Inorg. Chem.* **2001**, *40*, 4956. (f) Barbo, P.; Di Vaira, M.; Peruzzini, M.; Costantini, S. S.; Stoppioni, P. *Chem.—Eur. J.* **2007**, *13*, 6682. (g) Adolf, A.; Gonsior, M.; Krossing, I. *J. Am. Chem. Soc.* **2002**, *124*, 7111.
- (3) Wachter, J. *Coord. Chem. Rev.* **2010**, *254*, 2078.
- (4) (a) Biegerl, A.; Brunner, E.; Gröger, C.; Scheer, M.; Wachter, J.; Zabel, M. *Chem.—Eur. J.* **2007**, *13*, 9270. (b) Biegerl, A.; Gröger, C.; Kalbitzer, H. R.; Wachter, J.; Zabel, M. *Z. Anorg. Allg. Chem.* **2010**, *636*, 770.
- (5) Schwarz, P.; Wachter, J.; Zabel, M. *Eur. J. Inorg. Chem.* **2008**, 5460.
- (6) Guidoboni, E.; de los Rios, I.; Ienco, A.; Marvelli, L.; Mealli, C.; Romerosa, A.; Rossi, R.; Peruzzini, M. *Inorg. Chem.* **2002**, *41*, 659.
- (7) Kubicki, M. M. Personal communication.
- (8) Di Vaira, M.; Stoppioni, P.; Peruzzini, M. *J. Organomet. Chem.* **1989**, *364*, 399.
- (9) (a) Blachnik, R.; Wickel, U. *Angew. Chem., Int. Ed. Engl.* **1983**, *22*, 317. (b) Leiva, A. M.; Fluck, E.; Müller, H.; Wallenstein, G. *Z. Anorg. Allg. Chem.* **1974**, *409*, 215.
- (10) (a) Bues, W.; Somer, M.; Brockner, W. *Z. Naturforsch.* **1980**, *35b*, 1063. (b) Brockner, W.; Somer, M.; Cyvin, B. N.; Cyvin, S. J. *Z. Naturforsch.* **1980**, *36a*, 846.
- (11) Blachnik, R.; Wickel, U.; Schmitt, P. *Z. Naturforsch.* **1984**, *39b*, 405.
- (12) Raabe, I.; Antonijevic, S.; Krossing, I. *Chem.—Eur. J.* **2007**, *13*, 7510.
- (13) Biegerl, A.; Gröger, C.; Kalbitzer, H. R.; Pfitzner, A.; Wachter, J.; Wehrich, R.; Zabel, M. *J. Solid State Chem.* **2011**, *184*, 1719.
- (14) Balázs, G.; Biegerl, A.; Gröger, C.; Wachter, J.; Wehrich, R.; Zabel, M. *Eur. J. Inorg. Chem.* **2010**, 1231.
- (15) Bues, W.; Somer, M.; Brockner, W. *Z. Anorg. Allg. Chem.* **1984**, *516*, 42.
- (16) (a) Pfitzner, A. *Chem.—Eur. J.* **2000**, *6*, 1891. (b) Reiser, S.; Brunklaus, G.; Hong, J. H.; Chan, J. C. C.; Eckert, H.; Pfitzner, A. *Chem.—Eur. J.* **2002**, *8*, 4228. (c) Pfitzner, A.; Reiser, S.; Deiseroth, H.-J. *Z. Anorg. Allg. Chem.* **1999**, *625*, 2196. (d) Pfitzner, A.; Reiser, S. *Inorg. Chem.* **1999**, *38*, 2451. (e) Brunklaus, G.; Chan, J. C. C.; Eckert, H.; Reiser, S.; Nilges, T.; Pfitzner, A. *Phys. Chem. Chem. Phys.* **2003**, *5*, 3768.
- (17) (a) Qin, C.; Wang, X.; Wang, E.; Su, Z. *Inorg. Chem.* **2008**, *47*, 5555. (b) Carlucci, L.; Ciani, G.; Proserpio, D. M. *Coord. Chem. Rev.* **2003**, *246*, 247.
- (18) Peng, R.; Li, M.; Li, D. *Coord. Chem. Rev.* **2010**, *254*, 1.
- (19) Enjalbert, R.; Galy, J. *Acta Crystallogr., Sect. B* **1980**, *36*, 914.

- (20) Ghilardi, C. A.; Midollini, S.; Moneti, S.; Orlandini, A. *J. Chem. Soc., Chem. Commun.* **1988**, 1241.
- (21) Blacque, O.; Brunner, H.; Kubicki, M. M.; Leis, F.; Lucas, D.; Mugnier, Y.; Nuber, B.; Wachter, J. *Chem.—Eur. J.* **2001**, *7*, 1342.
- (22) SIR97, Altomare, A.; Burla, M. C.; Camalli, M.; Cascarano, G. L.; Giacovazzo, C.; Guagliardi, A.; Moliterni, G. G.; Polidori, G.; Spagna, R. *J. Appl. Crystallogr.* **1999**, *32*, 115.
- (23) Sheldrick, G. M. SHELXL-97. *Acta Crystallogr.* **2008**, *A64*, 112.